

## Modelling of High Precision Pneumatic Stepper Motors for Electronics and Modern Medicine Applications

Spartak Poçari<sup>\*a</sup>, Andonaq Londo<sup>b</sup>

Department of Energy, Faculty of Mechanical Engineering, Polytechnic University of Tirana, Albania

<sup>\*a</sup>[spocari@fim.edu.al](mailto:spocari@fim.edu.al); <sup>b</sup>[alondo@fim.edu.al](mailto:alondo@fim.edu.al)

### ABSTRACT

In this paper we will be focused on pneumatic stepper motors which offer a high precision in intermediate movements, as well as their electronic counterparts electronic stepper motors. This research work aims to build computer simulation models for high precision pneumatic stepper motor by analyzing their advantages and disadvantages. It has been analyzed the resistance to deformation and the level of stress for three types of materials such as plastic polylactic acid (PLA), 1060 aluminum alloy and A36 steel by using LabView and SolidWorks software's. Simulation results have shown that metallic materials have higher performance but when it comes to function within strong electromagnetic fields, plastic material definitely takes its place. These analysis results of the pressure signal propagation in the pipeline have determined that the length of the pipeline for pneumatic stepper motor should be minor than 3 m.

**Keywords:** Pneumatics, simulation, motor, optimization, modelling

### 1. INTRODUCTION

Many applications in the electronics and modern medicine industry require the use of pneumatic motors because these systems do not use electricity which can cause problems with induction but compressed air, and among their metal parts can be replaced with other non-metallic elements [1]. Pneumatic motors offer significant values of output force where most of them do not offer precision in intermediate movements [1-11]. In industry, the precise movements of components have a special importance, especially when it comes to robotic processes such as lathes and milling machines with numerical control, robotic arms in the electronics, pharmaceutical and modern medicine industries such as magnetic resonance imaging scanner [1, 11-14]. For small power and weight ratios these movements have been realized through stepper electric motors. The best option to use pneumatic stepper motors comes to areas where the effects of the magnetic field should be zero, as in the electronics industry, and in medicine application where the robotic arm can be in the effect of electromagnetic fields of scanners, as well as for high power and weight ratios.

Furthermore, stepper pneumatic motors can also be built with non-metallic materials for cases when the pneumatic motor works under the effect of strong electromagnetic field. They can have different dimensions depending on the power required at the

output. Figures 1 until 5 depicts different types of working principles of the stepper electric motors and stepper pneumatic motors [1-11].

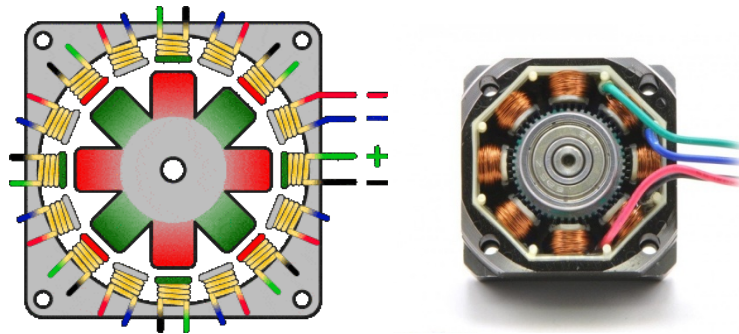


Figure 1. Working principle of stepper electric motors

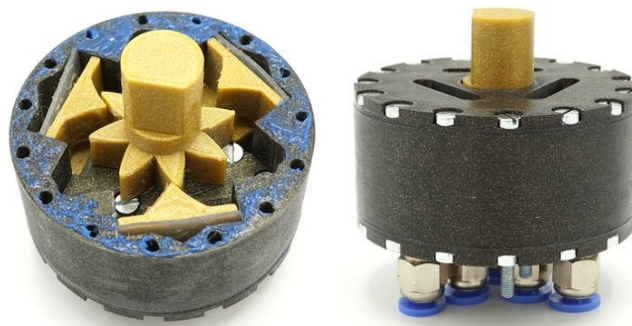


Figure 2. Working principle of stepper pneumatic motors

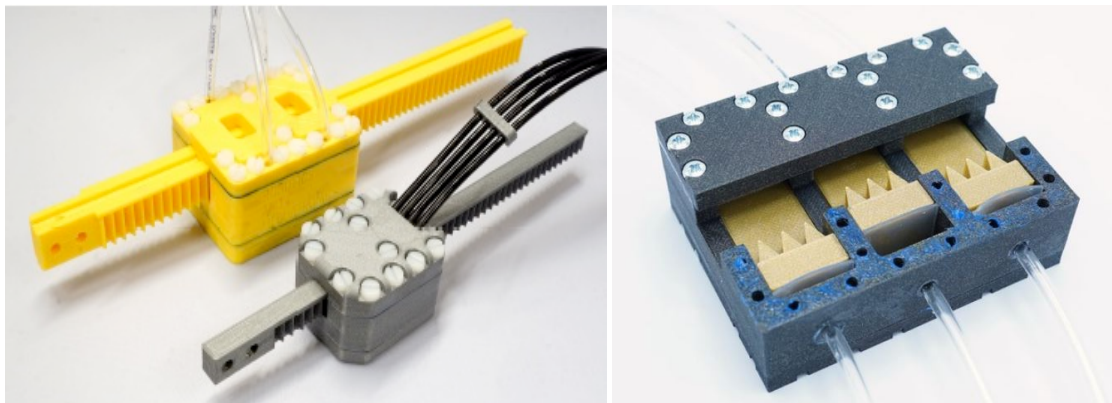


Figure 3. Working principle of linear stepper pneumatic motors [1]

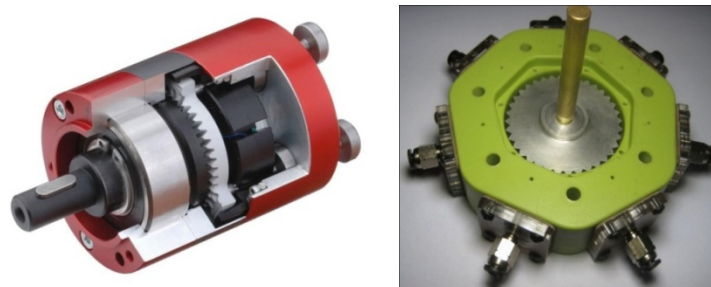


Figure 4. Stepper pneumatic motors, different construction with same working principle

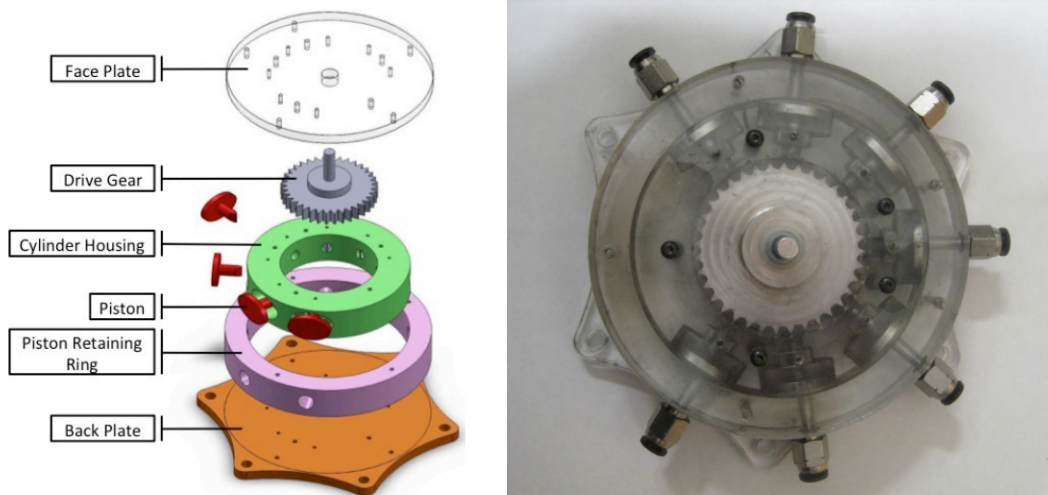


Figure 5. Exploded view of the R3 model pneumatic stepper motor [11]

Pneumatic step motors can also be built for linear motion as can be seen in linear pneumatic step motor of the above Figures 1 to 5 [1]. Even in these motors the working principle remains the same as that of rotary stepper motors.

In this paper we will be focused on pneumatic stepper motors which offer a high precision in intermediate movements, as well as their electronic counterparts electronic stepper motors. This research work aims to build computer simulation models for high precision pneumatic stepper motor by analyzing their advantages and disadvantages by proposing concrete solutions to improve their work.

## **2. MATERIALS AND METHODS**

In the previous research work it has been taken into account the application field where the dimensions and the value of the force required at the output of the pneumatic motor need to determine the necessary parameters for the pneumatic motor such as the field of electronics and medical where the material must be non-conductive and the dimensions should be less than 60 mm, precision accuracy 0.5 mm, applied force on 60 N and movement speed 6 mm/s [1]. In case of medical applications, the motor must operate without affecting the field of magnetic resonance of scanners and medical imaging equipment where the maximum control length can be 4 m. Furthermore, in other application area where the materials are metal, we should have the dimensions that can be depend on the power required at the output.

The working principle of stepper pneumatic motors is based on the use of precise linear movement of the piston at the beginning and end of the road where with the help of a toothed rotor they turn it into stepper rotational motion [1, 11]. The displacement step depends on the number of teeth that the toothed wheel has and the speed of movement depends on the number of pistons placed around the toothed wheel. To synchronize the movements these motors it is needed a set of solenoid valves commanded through a programmed electronic circuit.

Figure 6 and 7 depicts the motor model type R-64 pneumatic rotational stepper motor that we need to analyze in this research work. The R-64 is a powerful pneumatic rotary stepper motor which uses three pistons and are connected to an 8 or 16 gear [1]. Torque is large thanks to the piston surface with dimensions 24 mm x 24 mm. The external

dimensions of the engine were 33.35 mm x 33.35 mm x 29.8 mm.



Figure 6. Pneumatic stepper motor model R-64

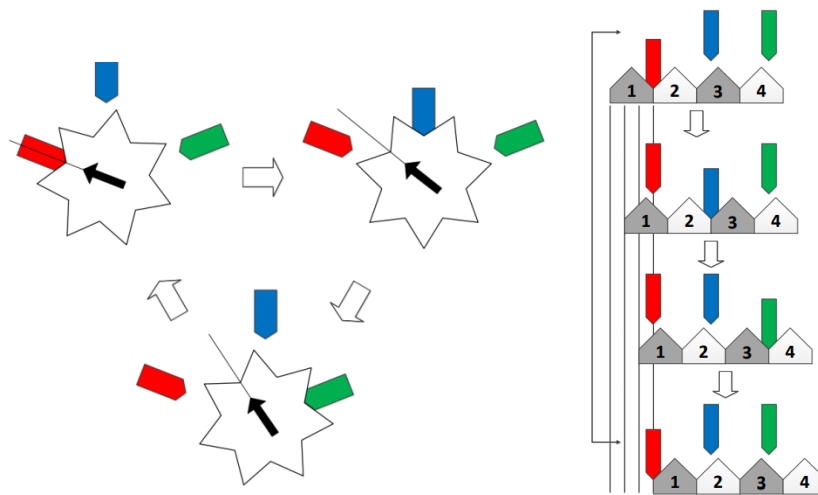


Figure 7. Phase principle for pneumatic rotary and linear stepper motor [11]

The design of pneumatic stepper motor is characterized by a number of variables like resolution ( $q$ ), angle between drive teeth ( $a$ ), number of teeth on the drive gear ( $n$ ), number of driving pistons ( $D$ ), outer radius of the drive gear ( $R$ ) and internal angle of gear teeth ( $B$ ). These variables are determined based on the power required at the output of the motor, the material and techniques that will be used for its construction as well as the response time of the solenoid valves. In order to analyze the working parameters, we have remodeled and printed pistons and toothed rotor of stepper motor by using 3D printer as can be seen in Figure 8. To realize the control of the engine pistons it has been used the set of pneumatic valves with electromagnetic control that are shown in the Figure 9. Based on it, the electro pneumatic valves for stepper motor control has been specified by using nominal standard airflow of  $Q=80$  L/min or  $Q=1.3$  L/s. The theoretical minimum time required to fill a cylinder bore  $V_c=38.6$  mL volume to a pressure of  $p=0.5$  MPa is calculated by equation (1).

$$\frac{p}{p_a} \cdot \frac{V_c}{Q} = \frac{0.5}{0.1013} \cdot \frac{38.6}{1300} = 146ms. \quad (1)$$

The required flow in the valve is calculated for tube length  $L_t$ , inner diameter  $d_t$  and cylinder bore volume  $V_c$ , the total air volume  $V_a$  associated with pressurizing one cylinder bore is expressed by equation (2) [1, 6]:

$$V_a = \frac{\pi}{4} L_t d_t^2 + V_c \quad (2)$$

With  $L_t = 3.0$  m,  $d_t = 4.0$  mm,  $V_c = 1.0$  mL, we have obtained from equation (2) the total air volume  $V_a$  that correspond to value 38.6 mL. With a step size of 1mm and a required velocity of 5 mm/s, a stepping frequency of 5 Hz is required. The average actual airflow through the valve is then  $5 \cdot 38.6 = 193$  mL/s, or 11.58 L/min. Given that instantaneous airflow through a valve depends on the pressure drop, and there are also delay and friction effects in the tube, the actual airflow requirement is higher than 30.2 L/min. Due to the limitation of the complexity of pressurization wave propagation dynamics, measurements were performed instead to assess the pressurization time of a selected valve.

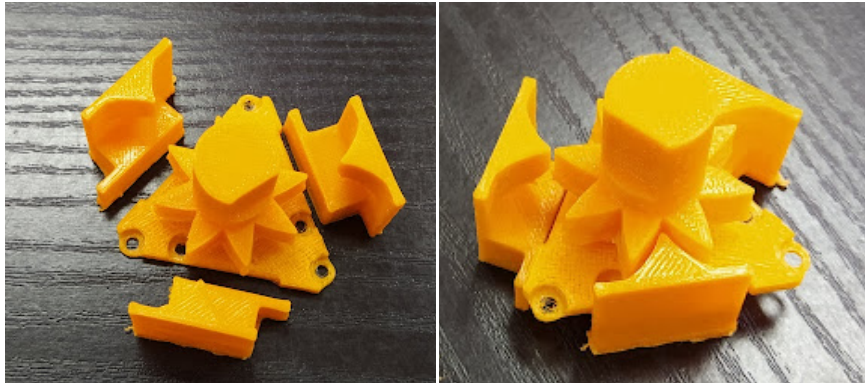


Figure 8. Pistons and toothed rotor of stepper motor printed with 3D printer



Figure 9. Electro pneumatic valves for stepper motor control

During the laboratory tests it was noticed that in the degree of precision of the pneumatic stepper motor several factors have a direct impact which are as follows:

- Stiffness of the piston teeth (resistance to deformation)
- The length of the tube that supplies the pistons of the motor
- The reaction speed of electromagnetic valves.

Based on the above factors we have analyzed the resistance to deformation and the level of stress by using the SolidWorks LabView software for three different types of materials such as plastic polylactic acid (PLA), 1060 aluminum alloy and A36 steel [15-17]. The pressure values that we have used in the piston cylinder chamber were approximately  $p = 5$  bar. Referring to the relation  $F = p \cdot S$  we have calculated the value of the force in the piston tooth by using equation (3) and correspond to the value 904.32 N.

$$S = \pi \cdot a \cdot b. \quad (3)$$

where  $a$  is the length of the piston surface with a value 24 mm and  $b$  is the width of the piston surface which correspond to the value 24 mm.

Figure 10 depict the analyzed effect of pipe length on the delay of propagation of the pressure signal for pipes with length  $L_1= 1.2$  m,  $L_2= 4.5$  m and  $L_3 = 10$  m. LabView software has been used to specially built the program for receiving the signal from the sensors [3].

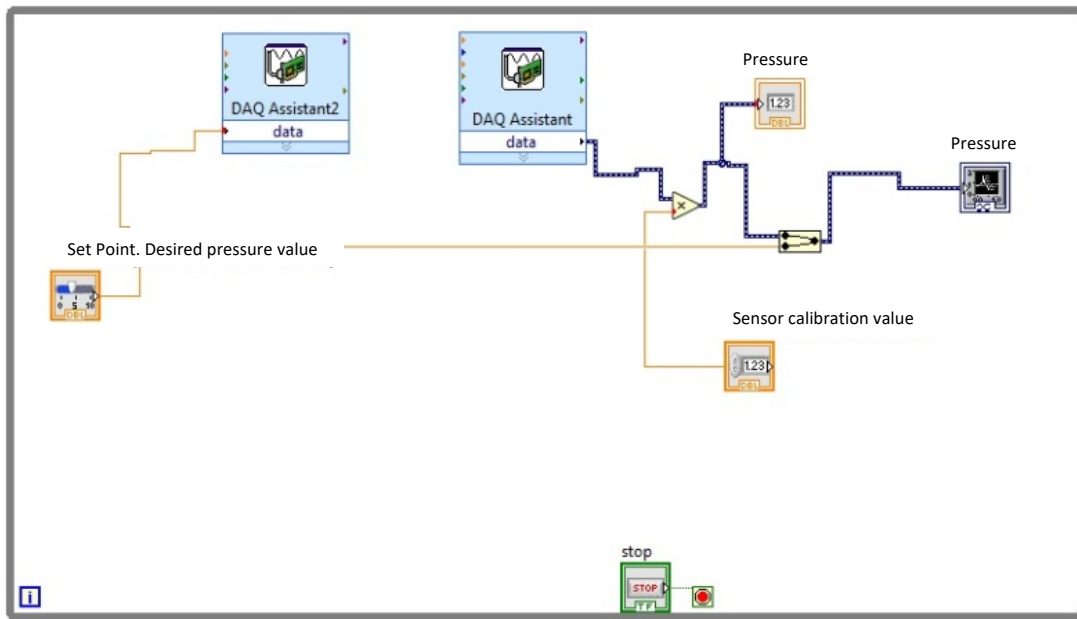


Figure 10. Effect of pipe length on the delay of propagation of the pressure signal for pipes with length  $L_1= 1.2$  m,  $L_2= 4.5$  m and  $L_3 = 10$  m, LabView software

The function block set point of the Figure 10 represents the desiderated pressure value given and has been connected with deploy data acquisition (DAQ) Assistant 2 function blocs that made possible to generate necessary amount of voltage to drive the pneumatic electro valve which generate e pneumatic signal. Afterward is measured through the pressure sensor and via the block of the DAQ Assistant function that has been entered into the program. Sensor calibration value has been used to ensure the propagation of the pressure signal through the pipe length. Then both signals will be displayed in the simulation results of section 3 at the Figure 17.

### 3. SIMULATION RESULTS

Simulation results for stress distribution for different materials are summerized in Table 1 and depicted in the Figures 11 until 16.

Table 1. Summary of simulation results in Solid Works

Piston Material	Max. Displacement in X Direction (mm)	Max. Rezultant Displacement (mm)	Max. Stress [N/m <sup>2</sup> ]
Plastic (PLA)	0.286	0.286	60,450,688.00
Aluminium 1060	0.009	0.009	63,809,460.00
A36 Steel	0.003	0.003	65,725,468.00

It has been shown in the Figure 11 and 12 the simulation results for plastic material (PLA) with the maximum deformation value which correspond to 0.286 mm and the maximum stress level to 60.4 MPa. For 1060 aluminum alloy material the simulation results of the Figures 13 and 14 has shown that the maximum deformation value reached the value 0.009 mm where the maximum stress level correspond to 63.8 MPa. In case of the A36 steel material the simulation results shown at Figures 15 and 16 has depicted that the maximum deformation value reached the value 0.003 mm where the maximum stress level correspond to 65.7 MPa.

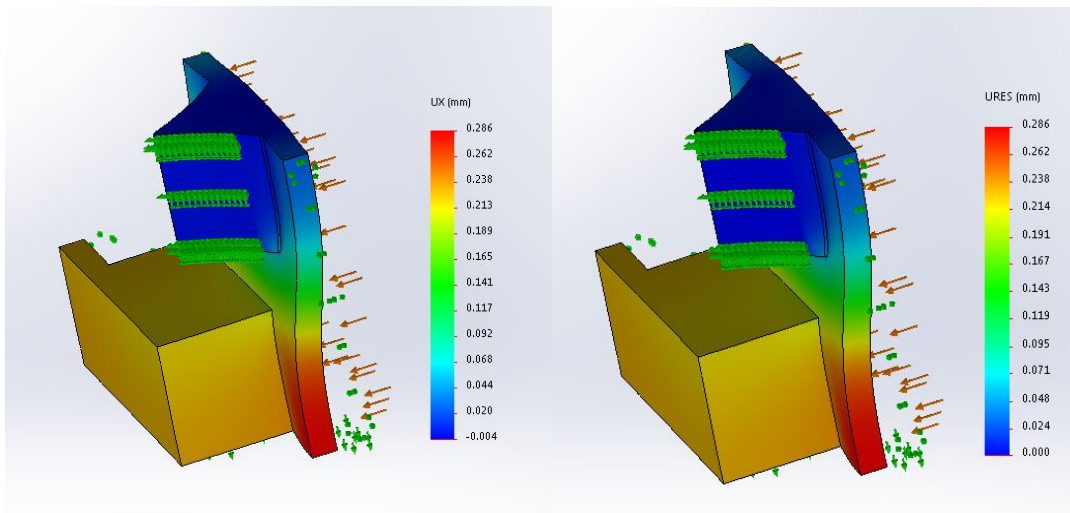


Figure 11. Deformation due to load  $F = 904.32\text{N}$  for PLA plastic material

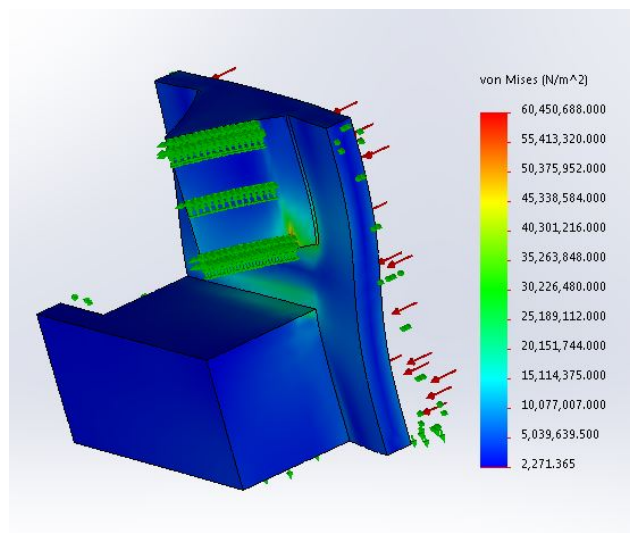


Figure 12. Distribution of stresses for  $F = 904.32\text{N}$  for PLA plastic material

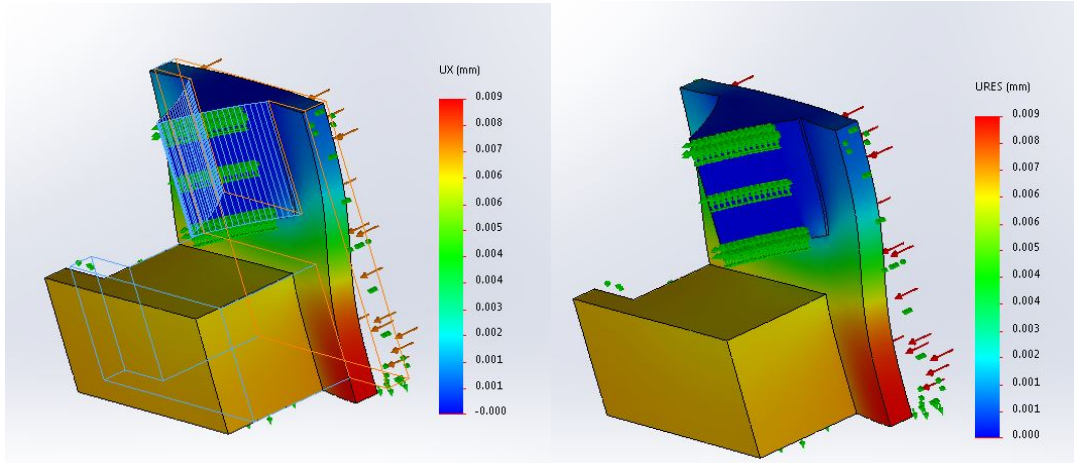


Figure 13. Deformation due to load  $F = 904.32\text{N}$  for 1060 Aluminum alloy material

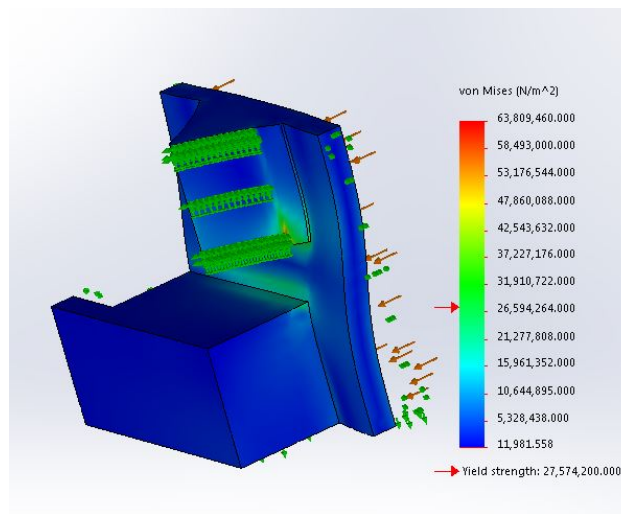


Figure 14. Distribution of stresses for  $F = 904.32\text{N}$  for 1060 Aluminum alloy material

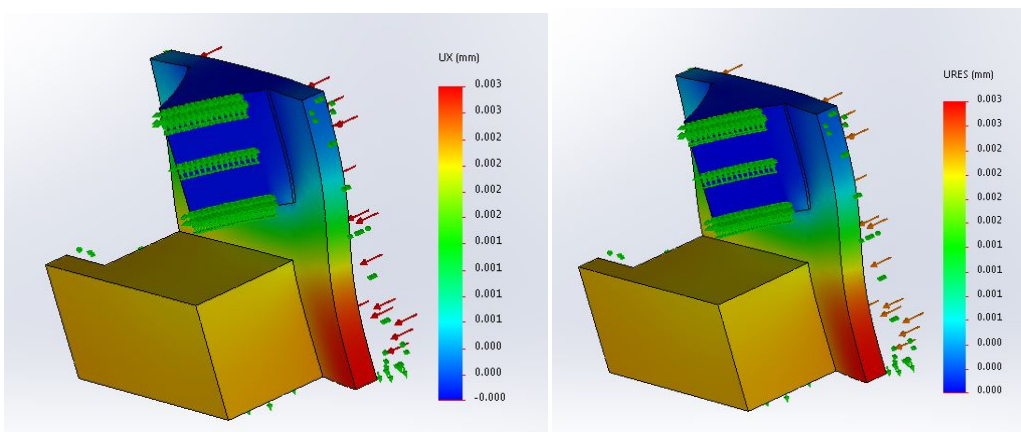


Figure 15. Deformation due to load  $F = 904.32\text{N}$  for A36 steel material

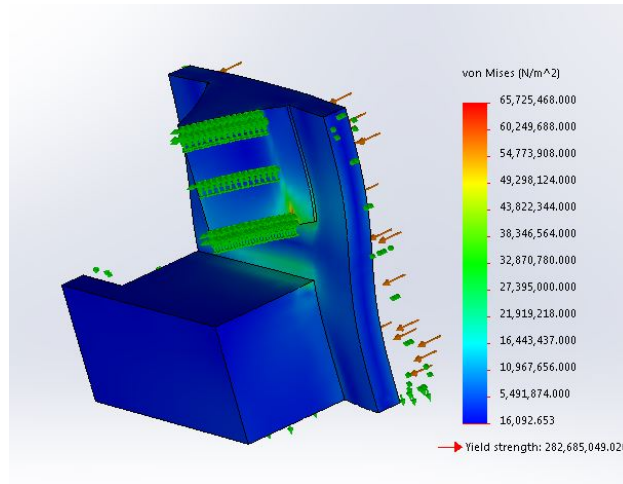


Figure 16. Distribution of stresses for  $F = 904.32\text{N}$  for A36 steel material

Furthermore, summary of the experimental results in relation to the effect of pipe length are shown in the Table 2 and Figure 17:

Table 2. Summary of experimental results in relation to effect of pipe length

Pipe length	Signal Delay
1.2 m	7 ms
4.5 m	16 ms
10 m	23 ms

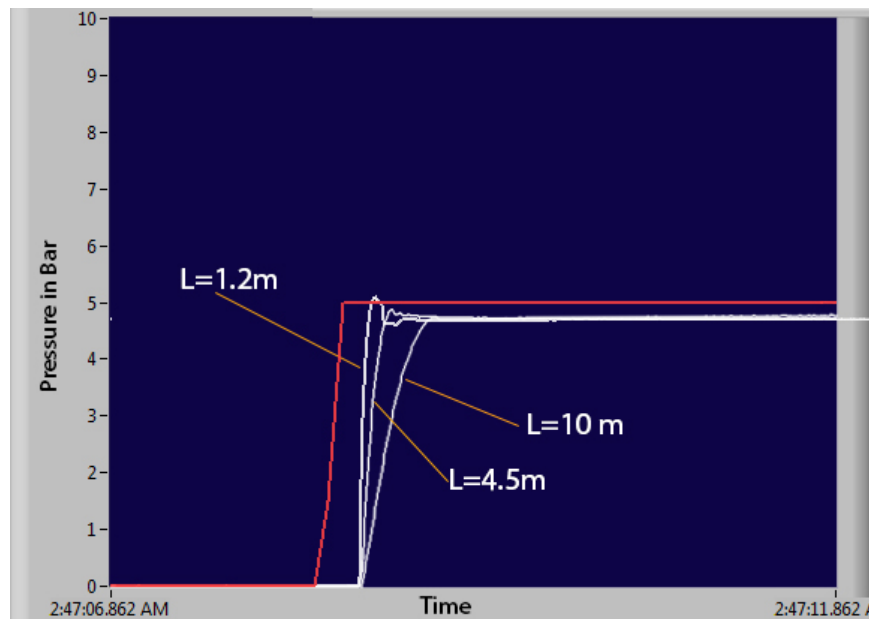


Figure 17. Effect of pipe length on the delay of propagation of the pressure signal

#### 4. DISCUSSION AND CONCLUSIONS

Many technological processes and medical industries require the application of precise movements with a high power / weight ratio. The use of pneumatic stepper motors is the optimal solution where there are many technological solutions for the realization of

precise movements of these motors. Based on it, our research work has been focused on the R-64 pneumatic rotational stepper motor model. The R-64 model offers simplicity in construction by considering power/weight ratio and depending on the purpose can be produced in plastic or metal materials.

It has been analyzed the resistance to deformation and the level of stress for three types of materials such as plastic material (PLA), 1060 aluminum alloy and A36 steel materials. From the analysis in stability for working pressures up to 5 bar the motor offers precise movement. In accordance to the size of the motor step which is 1 mm all three materials give an acceptable performance. It is understandable that metallic materials have higher performance but when it comes to function within strong electromagnetic fields, plastic material definitely takes its place. Regarding to the analysis of propagation of the pressure signal in the pipeline it has been seen that the length of the pipeline has a direct impact on the precision of these motors.

Based on our simulation results we can conclude that 1060 aluminum alloy and A36 steel materials can be used successfully in pneumatic stepper motor for different electronics applications. Furthermore, plastic materials (PLA) should be successfully replaced from the metallic element materials for pneumatic motors used in modern medicine industry. Also we can recommend that the length of the pipeline for pneumatic stepper motor in electronics and modern medicine applications should be minor than 3 m.

## CONFLICT OF INTERESTS

The authors would like to confirm that there is no conflict of interests associated with this publication and there is no financial fund for this work that can affect the research outcomes.

## REFERENCES

- [1] Groenhuis V., Stramigioli S. Rapid Prototyping High-Performance MR Safe Pneumatic Stepper Motors, *IEEE/ASME Transactions on Mechatronics*, 2018; 23(4); 1843-1853.
- [2] Londo A. (2008) Hydro pneumatics Transmission. 1<sup>st</sup> edition, *Sh.B.L.U Press*, Tirana, Albania.
- [3] Zecchi A. (1999) Controllo ed Elaborazione Numerica dei Segnali Con LabVIEW, *Tecniche Nuove Press*, Milano, Italy.
- [4] National Instruments (2016) BridgeView and LabView: G Programming Reference Manual. <https://www.ni.com/pdf/manuals/321296b.pdf>
- [5] Colombo N. (1985) Manuale dell'Ingegnere, *Politecnico di Torino Press*, Torino, Italy.
- [6] Parr A. (2011) Hydraulics and Pneumatics, 3<sup>rd</sup> edition, *Elsevier*, Netherlands.
- [7] Walters R.B. (1994) Sistemi di Regolazione Idraulici ed Elettroidraulici, *Tecniche Nuove*, Milano, Italy.
- [8] Griffiths D.J. (1999) Introduction to Electro Dynamics, *Prentice Hall Press*, New Jersey, USA.
- [9] Steidel R.F. (1989) An Introduction to Mechanical Vibrations', 3<sup>rd</sup> edition, *Wiley Press*, California, USA

- [10] SMC (2017) Electro Pneumatic Proportional Valve.  
<https://www.smcworld.com/products/en/get.do?type=GUIDE&id=VEF-VEP-E>
- [11] McDonald G., Overton G., Pastore K. (2011) Analysis and Performance of a Pneumatic Stepper Motor for Use in MRI Environments.  
[https://web.wpi.edu/Pubs/E-project/Available/E-project-010512-185427/unrestricted/Design\\_of\\_a\\_Pneumatic\\_Stepper\\_Motor\\_for\\_MRI\\_Environments\\_McDonald\\_Overton\\_Pastore\\_18Dec2012.pdf](https://web.wpi.edu/Pubs/E-project/Available/E-project-010512-185427/unrestricted/Design_of_a_Pneumatic_Stepper_Motor_for_MRI_Environments_McDonald_Overton_Pastore_18Dec2012.pdf)
- [12] Hysa G. and Meşe E. On the Behavior of Five-Phase Induction Motor Drive Under Normal and Faulty Conditions, *International Journal of Innovative Technology and Interdisciplinary Sciences*, 2021; 4(3); 754-763.
- [13] Pumwa J. Time Variant Predictive Control of Autonomous Vehicles: Time Variant Predictive Control of Autonomous Vehicles. *International Journal of Innovative Technology and Interdisciplinary Sciences*, 2019; 2(1); 62-77.
- [14] Minh V.T., Moezzi R., Dhoska K. and Pumwa, J. Model Predictive Control for Autonomous Vehicle Tracking. *International Journal of Innovative Technology and Interdisciplinary Sciences*, 2021; 4(1); 560-603.
- [15] Dhoska K. Tensile Testing Analysis of the HRB400 Steel Reinforcement Bar: Tensile Testing Analysis of the HRB400 Steel Reinforcement Bar. *International Journal of Innovative Technology and Interdisciplinary Sciences*, 2019; 2(3), 253-258.
- [16] Pramono A., Nugraha K., Suryana., Milandia A. and Juniarsih A. Design of Rolling Machine to Improve Mechanical Properties of Strapping-band Steel and Low Carbon Steel type SHP 440. *International Journal of Innovative Technology and Interdisciplinary Sciences*, 2022; 5(1); 822–832.
- [17] Pramono A., Dhoska K., Markja I. and Kommel L. Impact pressure on mechanical properties of aluminium based composite by ECAP-parallel channel. *Pollack Periodica*, 2019; 14(1); 67-74.